Simulation of a Blocking Event in January 1977[1]

K. Miyakoda, T. Gordon, R. Caverly, W. Stern, and J. Sirutis

Geophysical Fluid Dynamics Laboratory/NOAA, Princeton University, Princeton, NJ 08540

W. Bourke

Australian Numerical Meteorology Research Centre, Melbourne, Australia

ABSTRACT

January 1977 was a month noted for its extraordinary weather over North America. The winter was dominated by two persistent large amplitude ridges positioned over the west coast of North America and the Icelandic region of the Atlantic Ocean. A very intense trough reached deep into the eastern United States and caused one of the coldest Januaries on record. One-month integrations of various GCM's were conducted in order to test their ability to simulate this blocking event. Reasonably high resolution finite difference and spectral models available at GFDL were used. Each GCM was integrated from three different analyses of the initial conditions. For some models, a fairly accurate forecast was obtained and considerable skill was recognized in the simulation of the 30-day evolution in terms of the 5-day or 10-day mean flow fields, including the period of record breaking coldness over the eastern United States. The main conclusion is that proper treatment of the subgrid-scale processes as well as sufficient spatial resolution are essential for the simulations of this phenomenon as an initial value problem. Weak zonal wind poleward of about 40°N and upstream of the blocking ridge appears to be crucial for the successful simulation of the sustained blocking ridge.

1. Introduction

January 1977 was an extraordinary month weatherwise over the United States. The circulation was dominated by a persistent, large amplitude ridge over the Alaskan area, resulting in unusually high temperatures over the west coast and Alaska. Downstream in the Ohio Valley the monthly mean temperature was about 8-10°C below normal. On 27 January, the eastern United States experienced the most widespread record cold of the century.

It was thought that this would be an interesting case for a numerical simulation study. Starting with the initial condition on 1 January 1977 monthly prediction experiments were conducted, using atmospheric general circulation models (GCM) of reasonably high spatial resolution available at the Geophysical Fluid Dynamics Laboratory (GFDL). The objectives of this work were to simulate a real blocking phenomenon, to generate an example of dynamical one-month prediction, and to discover some clues concerning the mechanism of the blocking process.

It is sometimes argued that the limit of deterministic weather forecast is about two weeks and, accordingly, that the deterministic approach alone

could not produce a reasonable 30-day prediction. It was, however, our intention, motivated by the predictability studies (National Academy of Sciences, 1966; Smagorinsky, 1969), to assess whether some signal may still be distinguished from the noise, since one month is just beyond the limit of predictability. We feel if any individual forecast is to be successful, its five-day or ten-day time mean should still bear some resemblance to reality, even though the rms difference may have grown to a fairly large value. This reasoning is supported by the initial state perturbation experiment by Spar *et al.* (1978), in which small random errors did not change the model's monthly averaged climatology.

At the early stage of this project, a number of attempts to simulate the block which were made with an efficient spectral GCM all resulted in failure. In these forecasts, the mid-oceanic blocking ridge was pushed eastward and eventually washed out. The prognostic map at day 30 showed no resemblance to reality whatsoever. Substantial deviation often occurred as early as about day 10, and the forecast height pattern tended to be zonal. More than 10 one-month predictions were undertaken using two different analyses of the 1 January 1977 initial conditions and climatological or observed (climatology plus anomaly) external forcing by the sea surface temperature and snow deposit.

---

[1] Some portion of this paper was presented at the IUGG meeting at Canberra, Australia in December 1979.

After considerable frustration, we finally decided to use an expensive, i.e., high resolution finite difference GCM with improved subgrid scale (SGS) processes. The resulting prediction turned out to be good, without using anomalous external forcing. The most important factor for our success in this case was the inclusion of improved SGS processes into the GCM.

2. Description of models used in this study

Various versions of the GCM's employed in this study will be described. First, two types of numerical models were used, i.e., the N48L9 global finite difference model (Umscheid and Bannon, 1977), and the R30L9 global spectral transform model (Bourke, 1974; Bourke, et al. 1977; Gordon and Stern, 1974, 1982). Model N48L9 denotes the meridional resolution of the modified Kurihara grid, i.e., 48 grid points between a pole and the equator, and 9 vertical levels. Model R30L9 denotes rhomboidal spectral truncation at zonal wavenumber 30 and 9 vertical levels. Second, concerning the subgrid-scale physics, only two versions, i.e., and A2 and E4 will be used (Table 1) (see Miyakoda and Sirutis, 1977). The A2-physics is essentially the standard 1965 GFDL physics package (Manabe et al., 1965). The only modifications are that the soil moisture is predicted and the snow deposit is allowed to affect the surface albedo. The special features of E4-physics are incorporation of second order turbulent closure theory, elimination of "dry convective adjustment," adoption of the Monin-Obukhov process in the surface layer and inclusion of heat conduction through the soil.

It may be worthwhile to note that the lateral Austausch (an SGS process) calculation of heat, moisture, and momentum was parameterized by non-linear viscosity (Smagorinsky, 1963) in the N48L9 model and by either non-linear diffusion, as modified by Gordon and Stern (1982), or linear biharmonic (∇^4) diffusion in the R30L9 model.[2] For the parameterization of cumulus convection, the "moist convective adjustment" method was used in all models.

3. Verification of individual and ensemble mean forecasts

The predictions described in the rest of this paper were made without attempting to specify the external anomalous forcing. The initial conditions for soil moisture, snow deposit, and land-ice limit were adapted from the model's solution generated by the GFDL climate group (Manabe et al., 1974). Also, a

---

[2] The magnitude of the nonlinear viscosity is proportional to $(c\Delta)^2$, (Δ is the grid size), where $c = 0.25$ in the N48L9 model versus only 0.20 in the R30L9 model. The value of the coefficient for linear ∇^4 diffusion is $\nu \approx 2.68 \times 10^{15}$ m^4 s^{-1}. In effect, there is less lateral diffusion in the spectral model than in the grid point model.

TABLE 1. Physics difference between A2 and E4.

Processes	A2	E4
Vertical diffusion	Mixing length method, and dry convective adjustment	Turbulent closure method of hierarchy level 2.5 of Mellor-Yamada
Surface layer flux	Bulk aerodynamic method: transfer coefficient, C_D = 0.0043 land = 0.0011 sea	Monin-Obukhov similarity method, roughness, Z_0, 16.82 cm land, 0.032 u_*^2/g sea, (u_* is friction velocity)
Land subsurface process	None	Soil heat conduction

seasonally varying climatological sea surface temperature field was specified, following Alexander and Mobley (1976). The soil moisture and snow deposit in the subsequent days were predicted.

Although there is evidence that the initial conditions for wind, temperature and moisture are the dominant factors for the one-month range forecast (Shukla, 1981), the monthly simulation may require stochastic integrations or a Monte Carlo type approach (Epstein, 1969; Fleming, 1971; Leith, 1974) because it is beyond the limit of deterministic predictions. Therefore, three related initial analyses are prepared. However, in contrast to the usual Monte Carlo approach, these analyses possess systematic as well as random differences. The first and second are derived using the four-dimensional assimilation method developed at GFDL for 0000 GMT 1 and 2 January 1977, respectively. The third is the Hough function analysis (Flattery, 1971) of the National Meteorological Center (NMC), Washington, DC. for 0000 GMT 1 January 1977. NMC analyses are also used for verification.

In order to show the performance of the forecasts with various models, the verification scores are plotted in Fig. 1. The score is correlation coefficient of 10 day mean predicted versus observed geopotential height anomalies at 500 mb for the northern hemisphere poleward of 20°N, where the anomaly is defined as the departure from the climatological normal. The finite difference model is denoted by N or N48, and the spectral model by R or R30, and the physics is indicated by E or A.

The time mean scores for the first 10 days are high in all forecasts and then deteriorate rapidly for some models more so than in others. It is evident that the curves corresponding to the individual forecast of a particular model, e.g. the NE model, tend to be clustered together. Also the correlations for the individual forecasts are positive, at least for the NE, RE and NA models. These results suggest that the individual forecasts, e.g., NE1, NE2, and NE3 are not thoroughly contaminated by predictability decay. So far as the scores for the last 10 day mean and also for the last
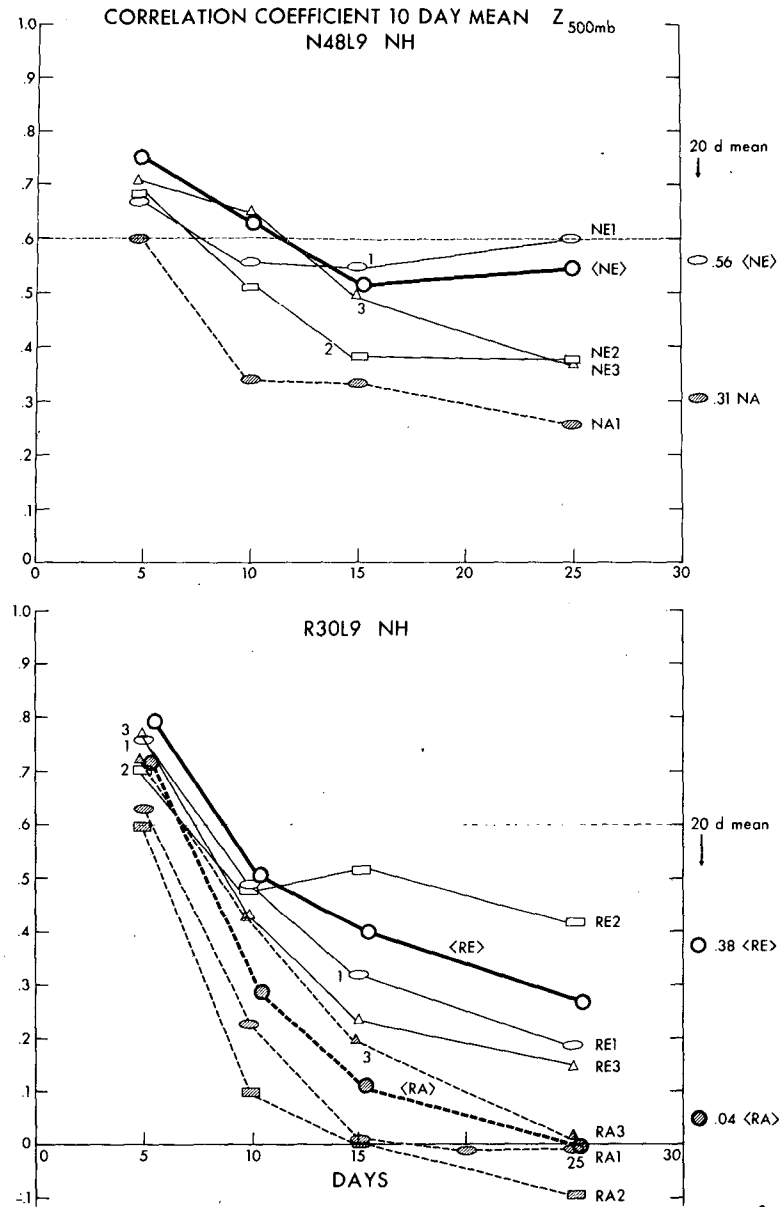
FIG. 1. The correlation coefficients between the various model forecasts and observation 500 mb geopotential height anomaly for the 10 day mean. Results for the three initial conditions are included, i.e., GFDL 1 January analyses (open oval), GFDL 2 January analysis (open rectangle), and NMC 1 January analyses (open triangle). The ensemble mean for the three realizations is indicated by the solid circle and the bracket. Correlation coefficients for the last 20-day mean of the ensemble average are shown in the column on the right hand side. The letter N indicates the finite difference model (upper), and R the spectral model (lower). The A-physics results are shown by dashed lines, and the E-physics results by solid lines. The horizontal line at a correlation coefficient of 0.6 is shown as a reference. According to ECMWF, this is the threshold value for practical usage of the daily prognoses.

20 day mean of January are concerned, the E-physics models invariably gave better forecasts than the A-physics models. This tendency is the same both for the N and R models. Another point is that, overall, the N models verify better than the R models.

4. Description of a successful simulation

One of the best predictions has been obtained with an N48L9-E4 (NE1) model. Figs. 2 and 4 compare the predicted and the observed maps of the 10–30
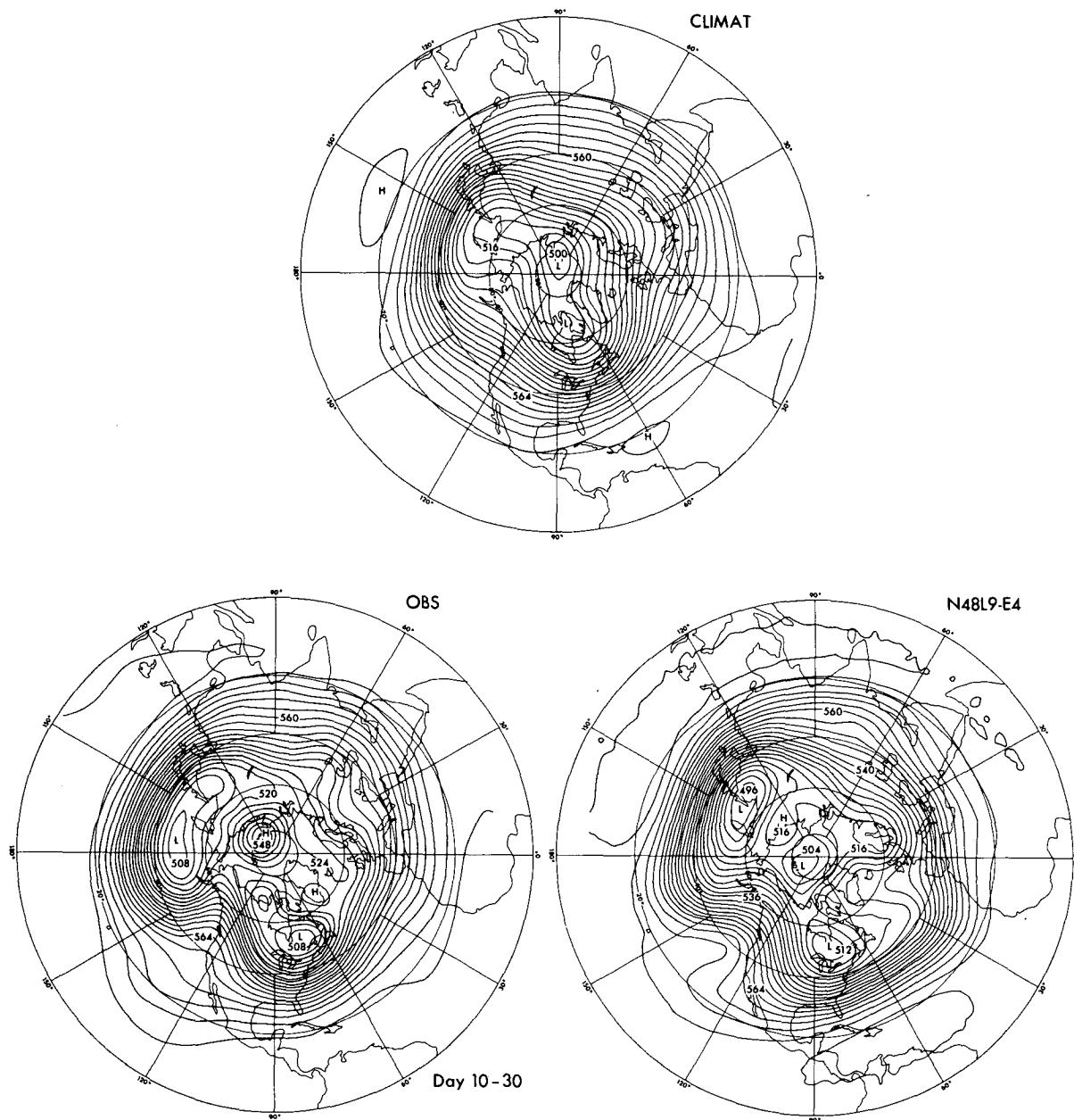
FIG. 2. The 500 mb geopotential height maps of January climatology (top), 10–30 day mean observation of NMC for January 1977 (lower left), the 10–30 day mean prognoses of the N48–E4 model (lower right). Contour interval is 40 m.

day averaged 500 mb geopotential height and sea level pressure, respectively. The first 10 days have been excluded since deterministic predictions can have some skill during that period. Also presented are the climatological mean maps for January. The corresponding maps of anomalies (i.e., departure from climatology) for the 1977 case are shown in Figs. 3 and 5.

The flow pattern during this month is characterized by large amplitude meandering westerlies and a strong blocking ridge over the eastern Pacific. This flow field does not exactly fit the definition of a classical blocking situation of Rex (1950, 1951) in the sense that a double jet structure in the meridional profile is not always present. But overall this flow field fits the definition of blocking by White and Clark (1975) rather well. The mid-latitude circulation has a sharp transition from zonal type flow upstream to meridional type downstream with the amplitude exceeding 5° of latitude. The longevity of the ridge was extraordinary, i.e., three months in this case (Wagner, 1977).
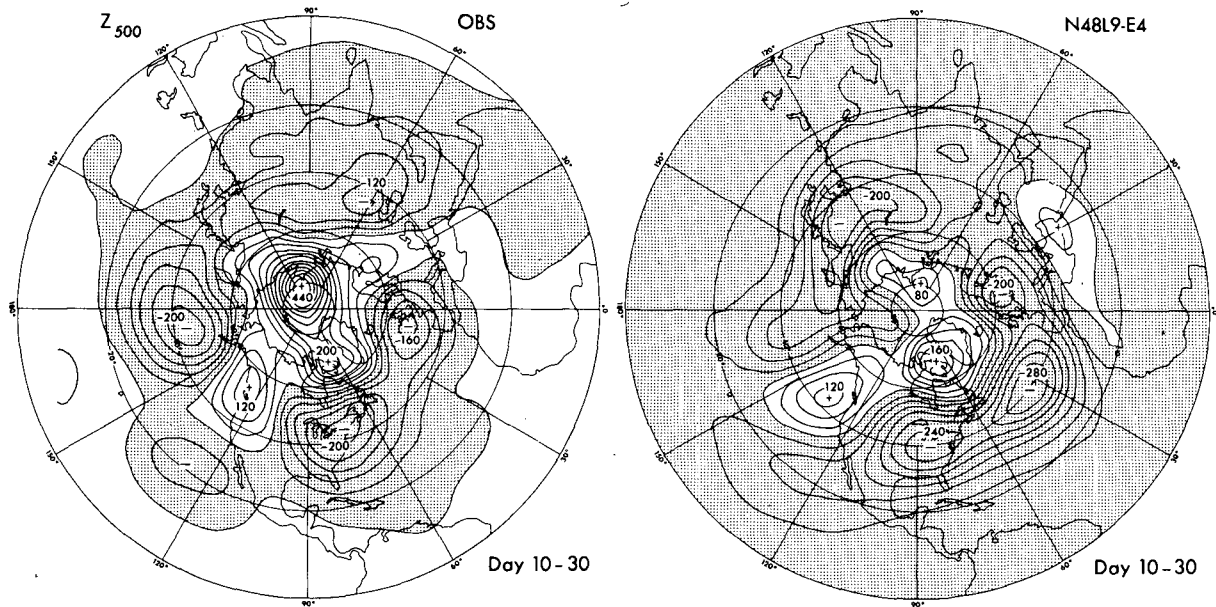
FIG. 3. The 10–30 day mean maps of the 500 mb geopotential height anomaly for NMC·observation (left) and the N48–E4 model forecast (right). Contour interval is 40 m. Negative anomaly areas are shaded.

Wallace and Gutzler (1980) have recently classified the northern hemispheric height patterns from 15 years of daily maps into five categories. The patterns in Figs. 2 and 3 precisely correspond to the "Pacific/North American" pattern of positive index in their teleconnection map classification. The most pronounced features of this category are the deep troughs over the northeastern Pacific (about 160°W), a strong ridge extending from the Pacific northwest of the United States to the Alaskan-Canadian border ~120°W[3] and another deep trough over the eastern part of North America at ~80°W. This is the case for January 1977 both in the observation and the prediction displayed in the preceding figures.

Yet there are discrepancies in the predicted patterns of geopotential height. The largest ones are the negative anomaly in the middle of the Atlantic Ocean at 500 mb and the negative anomaly in the middle of the Atlantic Ocean at sea level.

Fig. 6 shows the 20-day average 850 mb temperature field. The temperature distributions are on an orthographic projection with the nadir point at 45°N, 97°W. The severe coldness in the eastern part of North America was qualitatively reproduced in the forecast. However, Fig. 7 shows the predicted 20-day mean anomaly was 2.5°C lower than the observed. Similarly the unusual warmth over the west coast and Mexico was not correctly predicted. According to Namias (1978) the observed temperature anomaly

was in phase with the climatological mean position of the warm ridge. But the numerical simulation has not been successful in reproducing the correct position.

The prediction of rainfall is a most difficult quantity in the dynamical prediction. In this case, however, the simulation was not unreasonable (Fig. 8). The observed monthly precipitation (U.S. Dept. Commerce and U.S. Dept. of Agriculture, 1977) was below normal over the mid-west, and one of the driest Januaries on record occurred over the Pacific Northwest. Even so, several cities in those areas with record low temperature experienced some of their greatest January snowfalls (Wagner, 1977). The overall dryness was successfully reproduced in the prediction. In a normal year (climate in Fig. 8) there is a large amount of rainfall over the Mississippi and Ohio Valleys. This feature is often not well forecast (see Miyakoda and Strickler, 1981). But in January 1977, the precipitation was light and mostly confined in the Gulf states. The precipitation in the northeastern tip of the United States (New England) as well as the heavy lake-effect snow over Buffalo, New York, were not reproduced.

In the northwestern part of the United States, the predicted precipitation was excessive compared with the observation. This bias is associated with a series of predicted cyclones, which erroneously invaded inland from the Aleutian area. In reality, the cyclones were blocked by the Alaskan ridge.

Fig. 9 shows Hovmöller (time–longitude) diagrams for the 500 mb geopotential height in the zonal belt between 40° and 50°N latitude. In the non-blocking
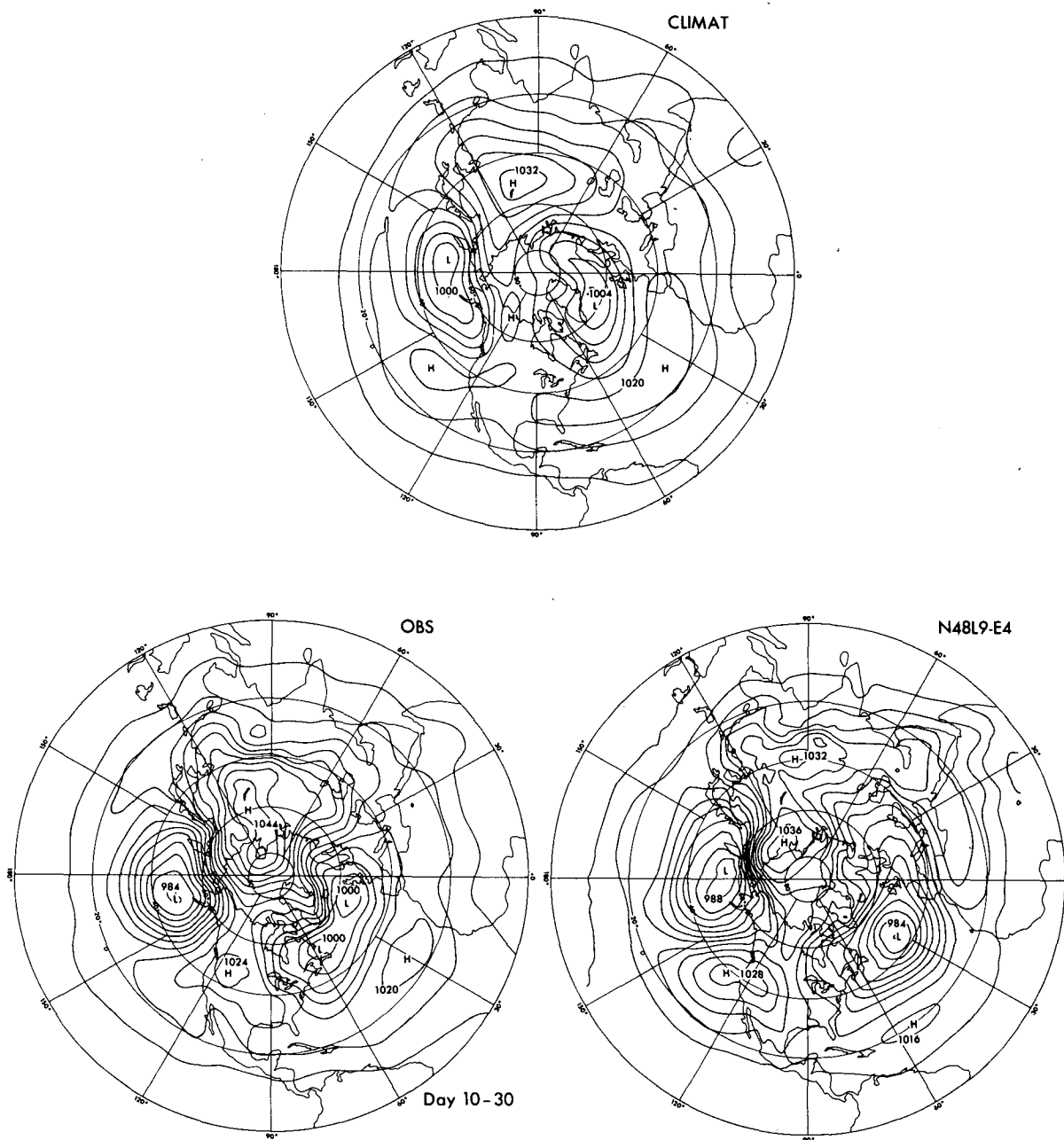
[3] White and Clark (1975) noted that blocking ridges are statistically at 170°W. The preferred regions of block during the 1976–77 winter, according to the analysis of observed data by Charney et al. (1981) is 130–180°W.

FIG. 4. Sea level pressure maps of January climatology (top), the 10–30 day mean observation of NMC for January 1977 (lower left), and the 10–30 day mean prognoses of the N48–E4 model (lower right). Contour interval is 4 mb.

situations, the pattern in the Hovmöller diagram would show a steady eastward displacement of the large scale troughs and ridges, whereas the chart in the case of 1977 indicates they are stationary.

Let us focus on the blocking ridge located at about 130°W. It is interesting to note that at the beginning of the forecast, the ridge has almost been "washed out," partially due perhaps to inappropriate initial conditions or incomplete initial balance. As mentioned by Edmon (1980) the Aleutian low was much stronger than normal. However, the ridge redeveloped later in the prediction at around day 6 and was well maintained throughout most of the one-month period.

It may be seen in the diagram of Fig. 9 that the stationary ridge is of a large scale, ~60° of longitude (White and Clark, 1975; Hartmann and Ghan, 1980). It may be a consequence of the ensemble of smaller scale travelling waves. The high pressure cells drifted slowly eastward, but new anticyclonic regions tended
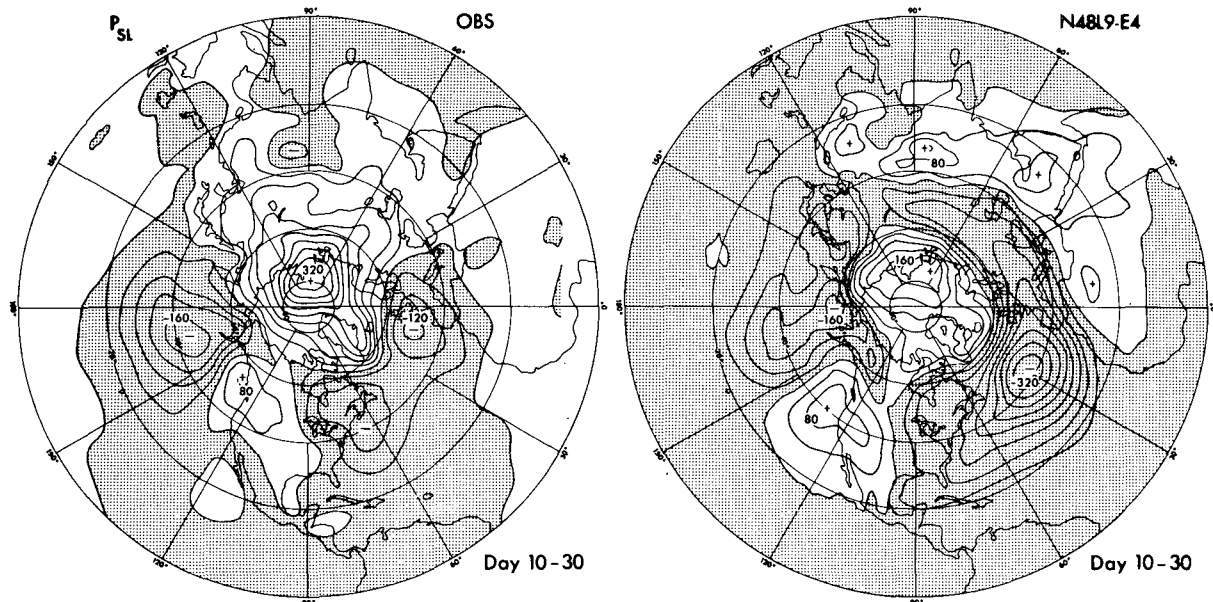
FIG. 5. The 10–30 day mean maps of the sea level pressure anomaly for the NMC observation (left) and the N48–E4 model forecast (right). Contour interval is 4 mb. Negative anomaly areas are shaded.

to reform on the west side of the block similar to the process discussed by Palmén and Newton (1969). In discussing his GCM results, Mahlman (1980) also observed that the blocking anticyclone appears to be sustained through the action of transient cyclonic disturbances. Lending to his argument, the dissipation of the transient cyclones leads to the irreversible deposition of warm, moist air with low potential vorticity in the region west of the blocking high, thus reintensifying the blocking pattern.

5. Comparison of successful and unsuccessful simulations

Taking the successful simulation NE1 (hereafter denoted by NE), and the unsuccessful simulation, RA1 (hereafter RA), the evolution of the respective flow patterns, vorticity distributions, and basic zonal flows are compared.

Figs. 10, 11 and 12 show the 10 day mean patterns of streamlines at 500 mb for the observation, the NE and the RA forecasts, respectively. The NE was successful in maintaining the blocking ridge throughout the month. On the other hand, the RA failed; the flow became more zonal, the amplitude of the ridge decreased and ridge position was displaced eastward.

The 40°N line in the diagrams is shown because blocking ridges are typically located poleward of this latitude. A solitary wave, manifested as a blocking ridge, cannot be sustained at lower latitudes due to the effect of wave dispersion (Yeh, 1949).

Fig. 13 shows the Hovmöller diagrams of the 500 mb geopotential height that are similar to Fig. 9 but

derived from the NA and the RA predictions. The NA was inferior to the NE (right in Fig. 9), and the RA was even worse. The Aleutian cyclones in the RA tended to be over-intensified (see Fig. 12) and they were advected eastward into the vicinity of the downstream blocking ridge. Each such transient disturbance could have transferred excessive energy into the Pacific jet itself, and later temporarily reduced the amplitude of the downstream ridge (Fig. 18 will show this feature). Also, the over-intensification of the jet over the eastern Pacific in the RA was so pronounced that the zonal wavenumber 1 turned out to be dominant in the monthly mean maps of the model prognoses, whereas in the observation the wavenumber 2 amplitude was large (Austin, 1980). Despite the possibility that the transient disturbances might act to reenforce the block the intense jet stream is unfavorable for maintaining it.

Fig. 14 is a comparative display of the evolution of the vorticity distribution at 500 mb. The region selected is the Pacific and North America sector, and the 10 day means of relative vorticity

$$\zeta = \frac{\partial v}{a \cos\varphi\, \partial\lambda} - \frac{\partial u}{a\, \partial\varphi}$$

are shown for three periods, i.e., days 0–10, 10–20 and 20–30.

The salient features, as revealed in the observation (the top three panels), are that the isolated negative vorticity indicated by blocking vorticity (encircled by thick lines) is located at the Alaskan and west Canadian coast area throughout the whole month and
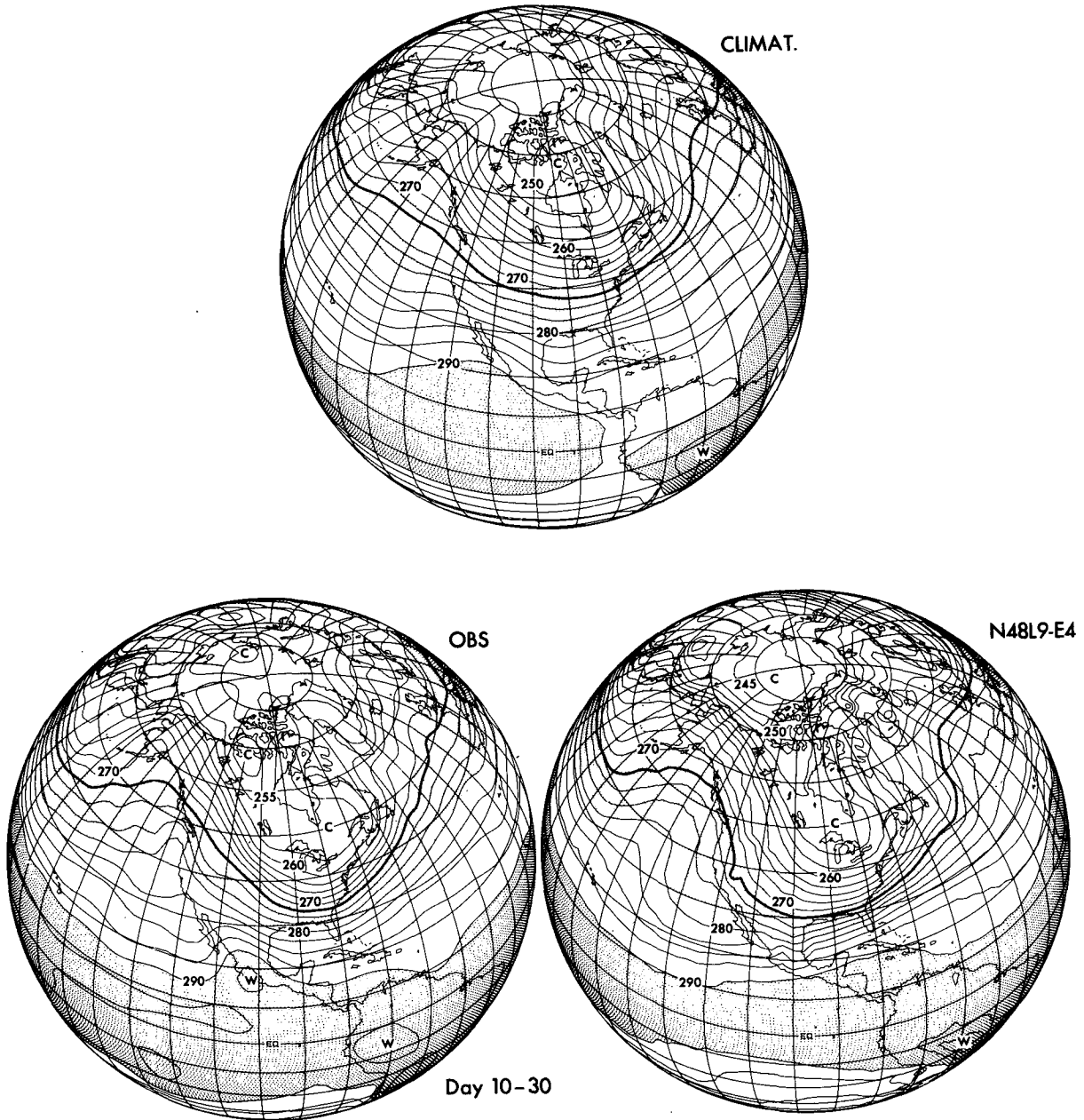
FIG. 6. The widespread record coldness over the United States for January 1977 is displayed by a 10-30 day mean temperature map at the 850 mb level. The predicted temperature shown is for the last 20 days of a one-month forecast (lower right) by the N48L9-E4 model, the observed temperature for the same period (lower left) and the January climatology (top). Units are deg. K, and the contour interval is 2.5 K.

that the *modon* type pattern (McWilliams, 1980), i.e., negative and positive vorticity centers which are juxtaposed meridionally as a pair, is found particularly in the observed map of day 10-20 (top). In other words, during this period split westerlies are observed. There is an area of anomalously intense negative vorticity near the North Pole. But it does not appear to affect the large scale distribution of vorticity.

Concerning the simulation, for the first 10 days, the NE as well as the RA have almost failed to maintain the blocking vorticity. In the period day 10-20, however, the blocking vorticity has been regenerated in the NE whereas it has not in the RA. In general, the RA vorticity distribution tends to be rather zonally symmetric throughout the month.

Fig. 15 displays the 30-day mean of zonally aver-
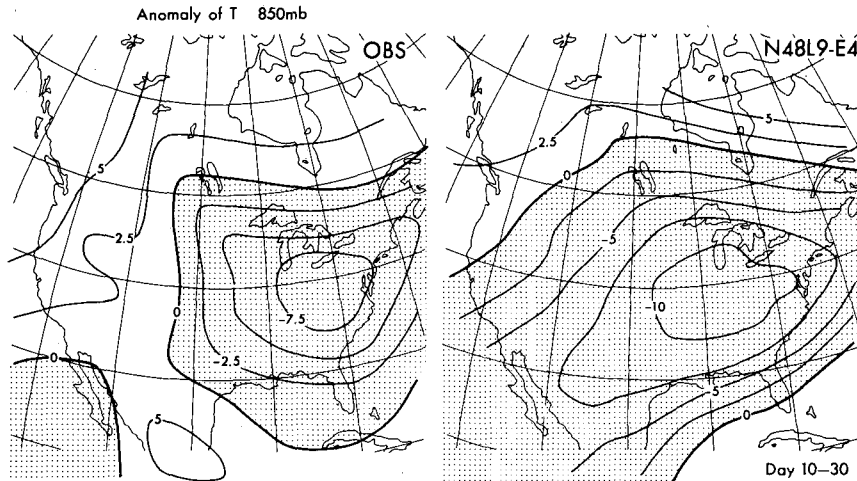
Anomaly of T　850mb

FIG. 7. The 10–30 day mean 850 mb temperature anomaly maps over North America for the NMC observation (left) and the N48–E4 model forecast (right). Contour interval is 2.5°C.

aged zonal wind at various levels, for the NE and the RA predictions. The observation and January climatology are also plotted. The observed tropospheric jet over the Pacific and Atlantic was abnormally strong and it was displaced to the south of its usual position (Edmon, 1980). Such abnormally strong zonal flow over the Pacific was also experienced in another case of anomalous blocking, i.e., January 1963. On the other hand, according to a study of year-to-year variability in autumn/winter blocking ridge activity by White and Clark (1975), the ridges are intense in the years when the surface wind and the thermal wind (difference between 47.5° and 32.5°N) in the lower troposphere are both weaker than normal (the correlation is −0.78). As will be discussed later, it is possible that the intense blocking ridge is a consequence of what may be called local resonant interaction. If so, weak zonal westerlies are again favorable for blocking. Thus, there is an apparent contradiction between the observed wind speed and that which is favorable for blocking. It can be reconciled, however, by the fact that the observed zonal winds north of ∼42°N in Fig. 15 were considerably weaker than normal. As seen in Fig. 14, the main track of positive vorticity and the blocking negative vorticity were located at the zonal belt of about 50°N. The belt of weak westerlies corresponds to this latitude. A southward shift of the westerly maximum in January 77 relative to climatology and the existence of considerably weaker westerlies north of 42°N relative to climatology appear to be crucial concurrent features for the maintenance of the North Pacific ridge. The NE model was able to simulate these key features satisfactorily, whereas the RA model was not. In particular the accurate latitudinal position of the zonal wind maximum in the NE calculation is significant.

One of the measures to assess the degree of meandering westerlies is the eddy kinetic energy, K_E, i.e., the energy of the departures from the zonal mean wind components. A particularly appropriate measure for the blocking activity may be the stationary component of the eddy energy, (K_{SE}), which is to be distinguished from the transient component, (K_{TE}). Latitude profiles of K_E are shown in Fig. 16, where the stationary component is the monthly average in our case, and the transient component is the deviation from the former. Vertically integrated values have been plotted.

The observed eddy kinetic energy for January 1977 was extraordinarily large, as is typical of the blocking situation (see January 1963 case, Krueger et al., 1965). The K_{SE} that is related to the blocks is associated with the second peak at ∼50°–60°N. Fig. 16 indicates that the NE model produced a large amount of stationary energy, similar to observation. On the other hand, the RA model generated less stationary energy. The reason for the achievement of the NE model with respect to the eddy kinetic energy is discussed elsewhere.

6. Discussion of possible favorable effects

a. The qualification of GCM's

Over the years, there have been a number of attempts at numerical simulation of blocking processes with GCM's, including Kikuchi (1969; 1971; 1979) and Lejenäs (1977). Also, Everson and Davies (1970) and others (see Davies, 1978) have used simpler models. These works successfully simulated aspects of blocking ridges. Invariably it was concluded that the presence of mountains is most important and that the land–sea contrast or the longitudinally varying heat sources are desirable.
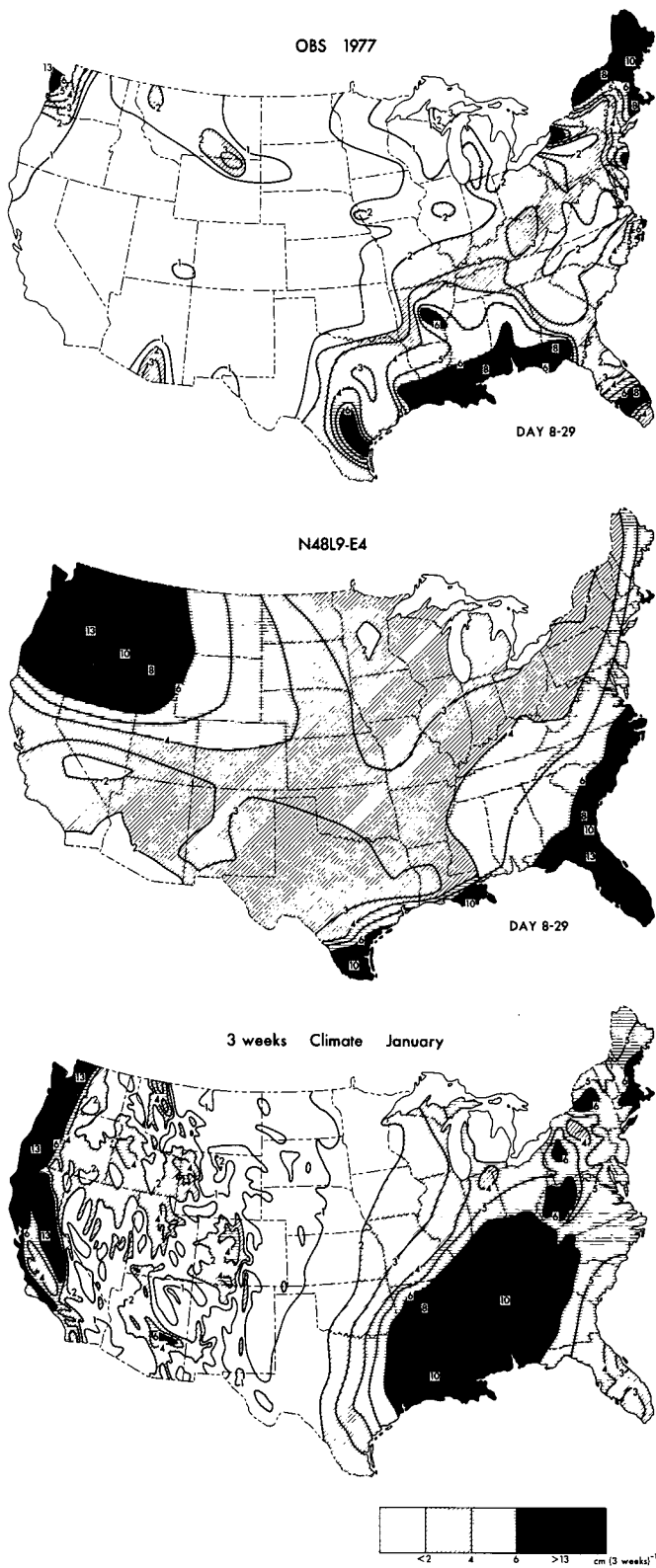
OBS 1977

DAY 8-29

N48L9-E4

DAY 8-29

3 weeks   Climate   January

<2   4   6   >13   cm (3 weeks)⁻¹

FIG. 8. The precipitation distributions of the 8–29 day mean obser-
vation of January 1977 (top), the 8–29 day mean prognoses of the N48–
E4 model (middle) and January climatology (bottom). Units of contour
values are centimeters (3 weeks)$^{-1}$. The scale of precipitation is indicated
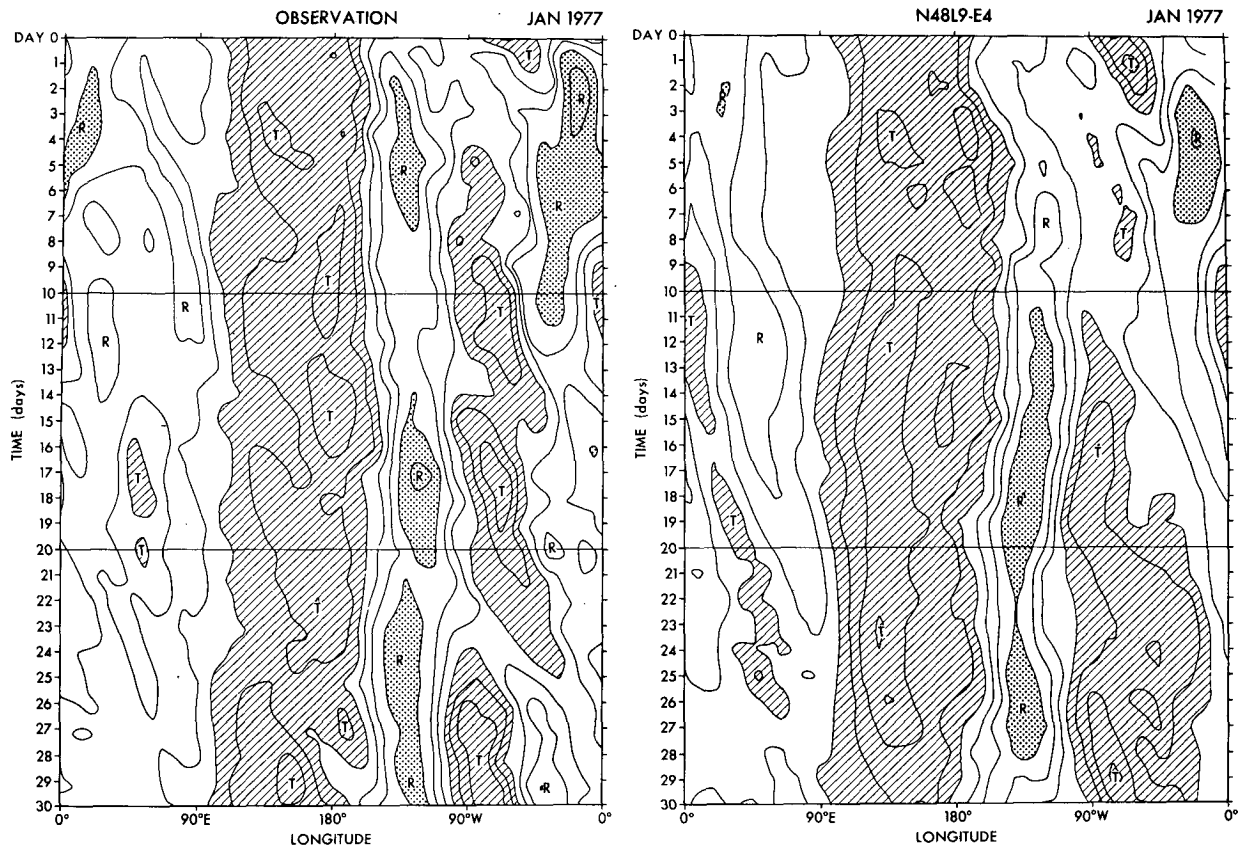by the legend at the bottom.

855

FIG. 9. Time–longitude charts (Hovmöller) of the 500 mb geopotential heights between 40 and 50°N for the observation (left) and the N48L9–E4 forecast (right). Ridges and troughs are marked by R's and T's. The dense stippled areas are those with height > 5640 m, and the coarse stippled areas are those with height < 5280 m.

In our case, reasonable orography and land–sea contrast were already included, and yet our experiment indicates that these effects alone were not sufficient to simulate blocking. The reason for the difficulty in our case is that we treated the real blocking situation as an initial value problem, starting from real data. Hence, both the model's ability to forecast the evolution of transient states (or being able to maintain an existing pattern in a blocking situation) as well as its climatology are crucial. In any case, it does appear that SGS processes are key factors in bringing about a successful numerical simulation of a block, at least in the case of January 1977. For example, the role of the E4 versus A2 physics is evident in a comparison of the NE versus NA and RE versus RA forecast results (see Appendix). Lateral diffusion is another potential factor. The R30 lateral diffusion may have been too weak to dampen transient cyclonic disturbances over the central Pacific before they transferred considerable energy into the Pacific jet or later destructively interfered with the stationary ridge downstream. Also, the linear ∇^4 diffusion is too scale-selective to directly affect the Pacific jet, despite the jet's narrow width.

There could be other factors. Bengtsson (1981) pointed out that the very high resolution models manage, in a remarkable way, to predict a blocking event in great detail even beyond one week. This point was also experienced in the GFDL experiments. In fact, the superior performance of the finite difference model (compared to the spectral model) could be due to its finer, spatial resolution. According to an extensive study involving the comparison of the medium-range forecasts made with the spectral and the finite difference models (Jarraud et al., 1981), the N48 model is equivalent to the T53 ≈ 63 spectral model in terms of degrees of freedom for the horizontal representation as well as the practical capability of forecasts, where T53, for example, denotes triangular truncation at wavenumber 53. The T53 ~ 63 resolution corresponds to R38 ~ 44, and, thus, the R30 model clearly has coarser resolution than the N48.

Yet another factor is model topography. Recently, Wallace et al. (1983) have found that a delicate difference of orography could generate serious systematic errors in the forecasted height field by a GCM. They used the so-called envelope mountain and ob-
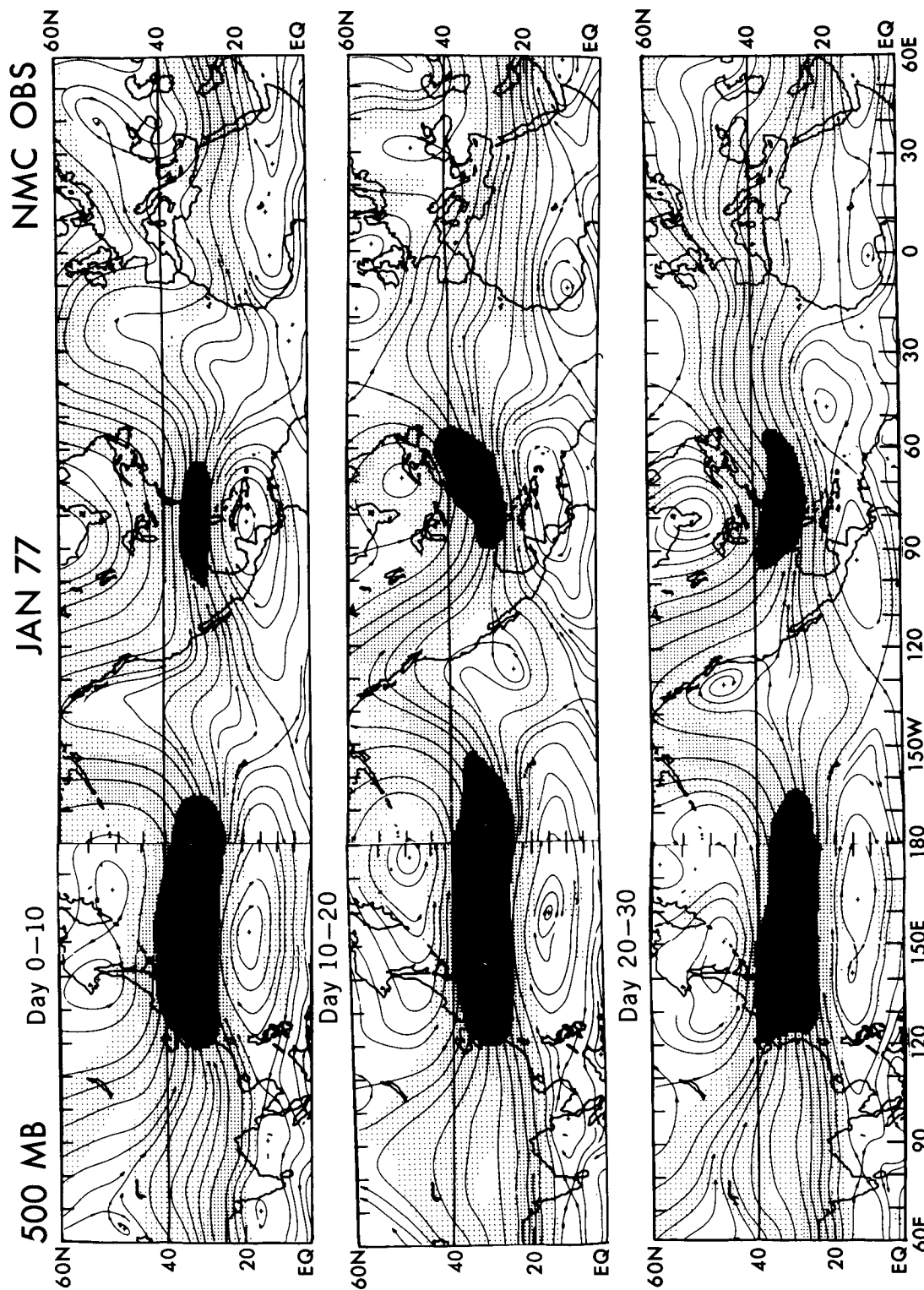
FIG. 10. The NMC observed wind fields are shown by 10-day mean streamlines at 500 mb in the northern hemisphere between the equator and 60°N latitude for, day 0–10 (top), day 10–20 (middle) and day 20–30 (bottom). Heavy shade denotes winds > 60 kt, medium shade denotes winds between 60 and 40 kt, and light shade denotes winds between 40 and 20 kt. The line at 40°N is shown as reference.

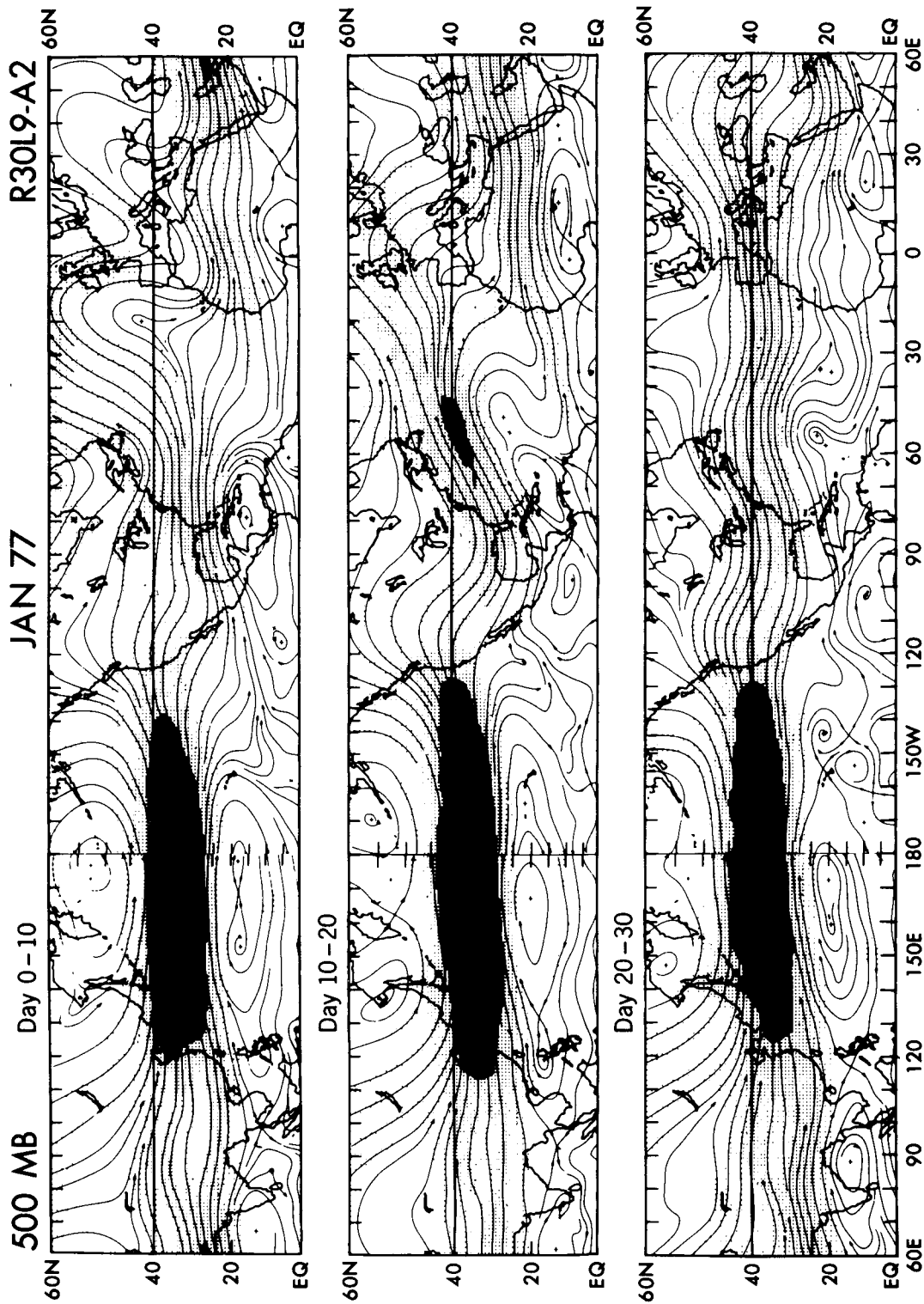FIG. 11. As in Fig. 10, but for forecasts by the NE model.

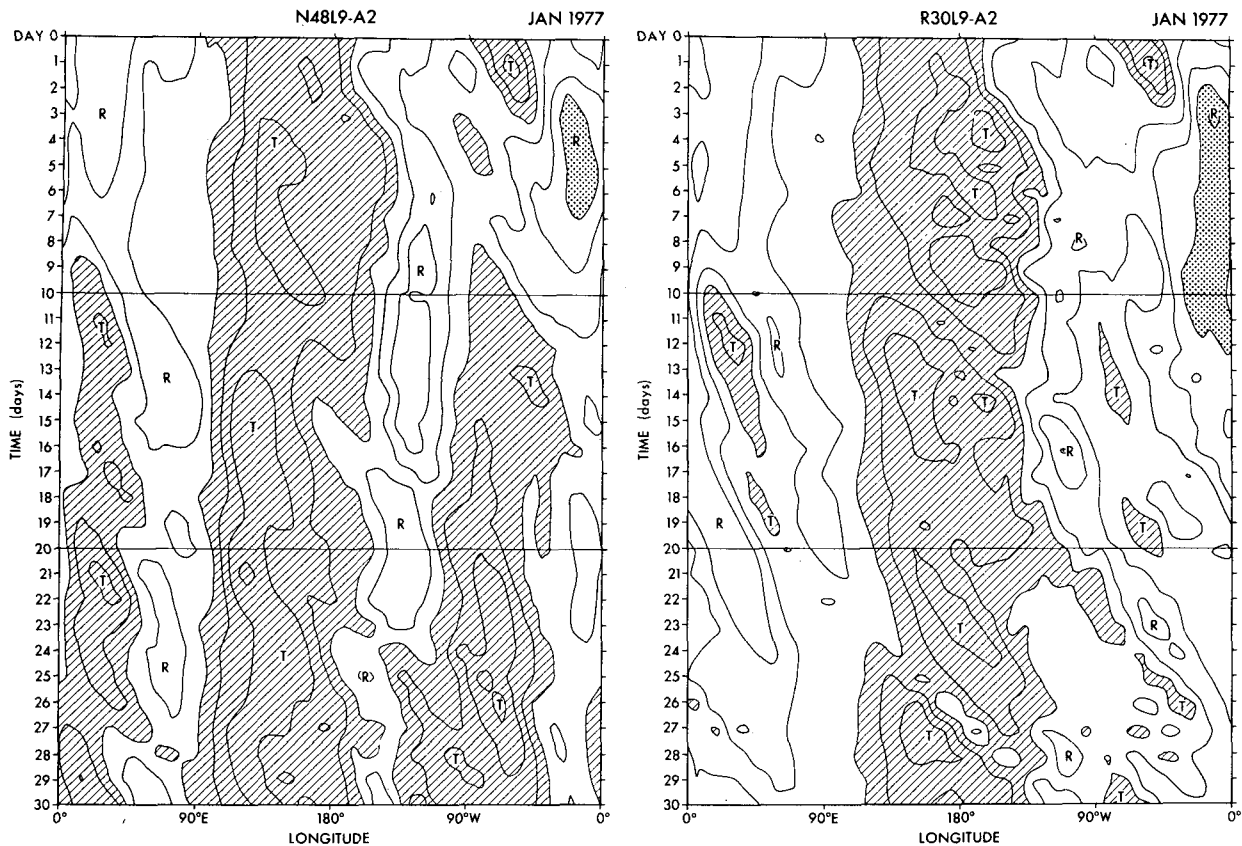FIG. 12. As in Fig. 10, but for forecasts by the RA model.

FIG. 13. Time–longitude charts (Hovmöller) of the 500 mb geopotential heights for the NA forecast (left)
and the RA forecast (right). See caption of Fig. 9.

tained improved forecasts for large-scale patterns. Stimulated by this finding, we compared the heights of the N48L9, versus R30L9 topographies *a posteriori*. No systematic bias was found globally. However, over the central Rockies the R30 topography had a more extreme gap (by 400 m) than the N48. This situation may be relevant to the amplitude of the Pacific/North American type of blocks. The Rockies should relatively decelerate the zonal flow, due to their predominantly north–south orientation. But for jets flowing over the Rockies in the vicinity of the gap, the deceleration would be less, particularly in the case of a more extreme gap. Curiously, the R30 jet crosses the Rockies in the vicinity of the gap, consistent with, but not proof of the hypothesis.

In the NE forecasts, the geopotential height or pressure over the Arctic region was not well predicted (see Figs. 2, 4 and 11). Quiroz (1977) has speculated that the observed high pressure was a consequence of descent associated with stratospheric sudden warming (beginning 6 December 1976 and reaching a maximum temperature around 3 January 1977 at the 10 mb level). Taylor and Perry (1977) and O'Neill and Taylor (1979) also pointed out the vertical con-

tinuity of anomalously high polar temperature and easterly winds from the surface up to at least the 10 mb level, but cautioned against making a hasty determination of any causal relationship. We speculate that a model with finer vertical resolution model may be required in order to make a better simulation for the Arctic region.

b. External (anomaly) forcings

In our experiments, the blocking was reproduced, to a reasonable extent, without using the anomalies of sea surface temperature or the snow-albedo. Namias (1978), however, postulated these were among the possible "multiple-causes" for the anomalous January 1977 circulation. The anomalously warm sea surface temperature, in the El Nino region, could be especially important (White and Clark, 1975; Horel and Wallace, 1981; Hoskins and Karoly, 1981; Simmons, 1981). By the same token, anomalous soil moisture and snow deposit could also be relevant (Namias, 1978; Austin, 1980, for example).

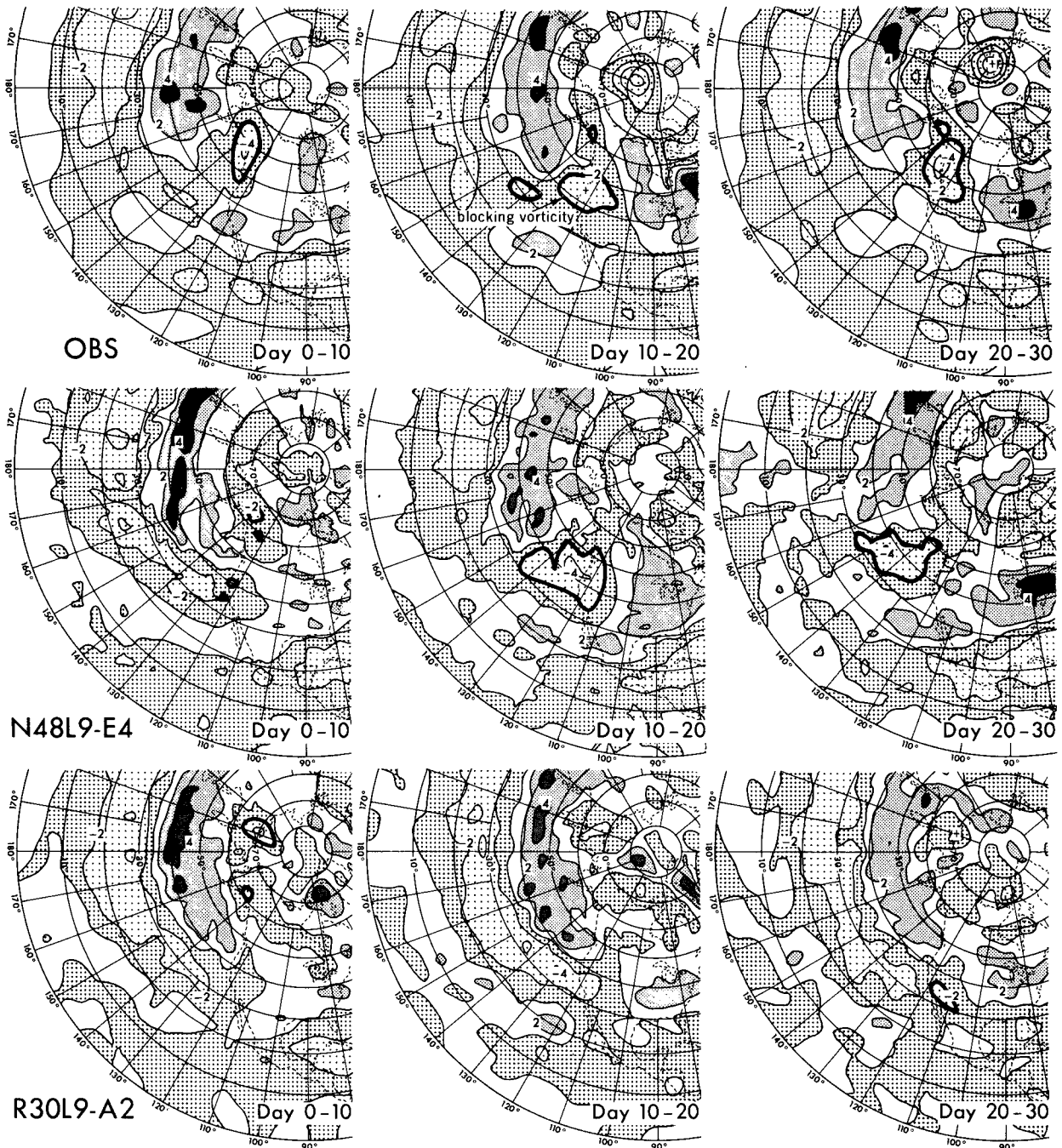In the case of 1977, the phases of the anomalously intense planetary scale waves happened to coincide

FIG. 14. Vorticity distribution over the North Pacific and North America sector in the three 10-day periods for observation, the NE and the RA models. Contour interval is 2×10^{-5} s^{-1}. Positive vorticity areas with intensity $> 2 \times 10^{-5}$ s^{-1} are stippled, and negative vorticity areas with intensity $< -2 \times 10^{-5}$ s^{-1} are shaded. Key negative vorticities in the blocking area are contoured by thick lines.

with the climatological mean positions. There is evidence that at one month, the forced mode solution due to the anomalous ocean temperature is similar to the solution using climatological sea temperature forcing, as shown in Fig. 3 of Miyakoda and Chao

(1982). However, in order to discuss the real causes of blocking, it may be necessary to distinguish situations by the time scales involved. Blocking episodes on the order of three months, for example, probably can only be explained by the anomalous effects of
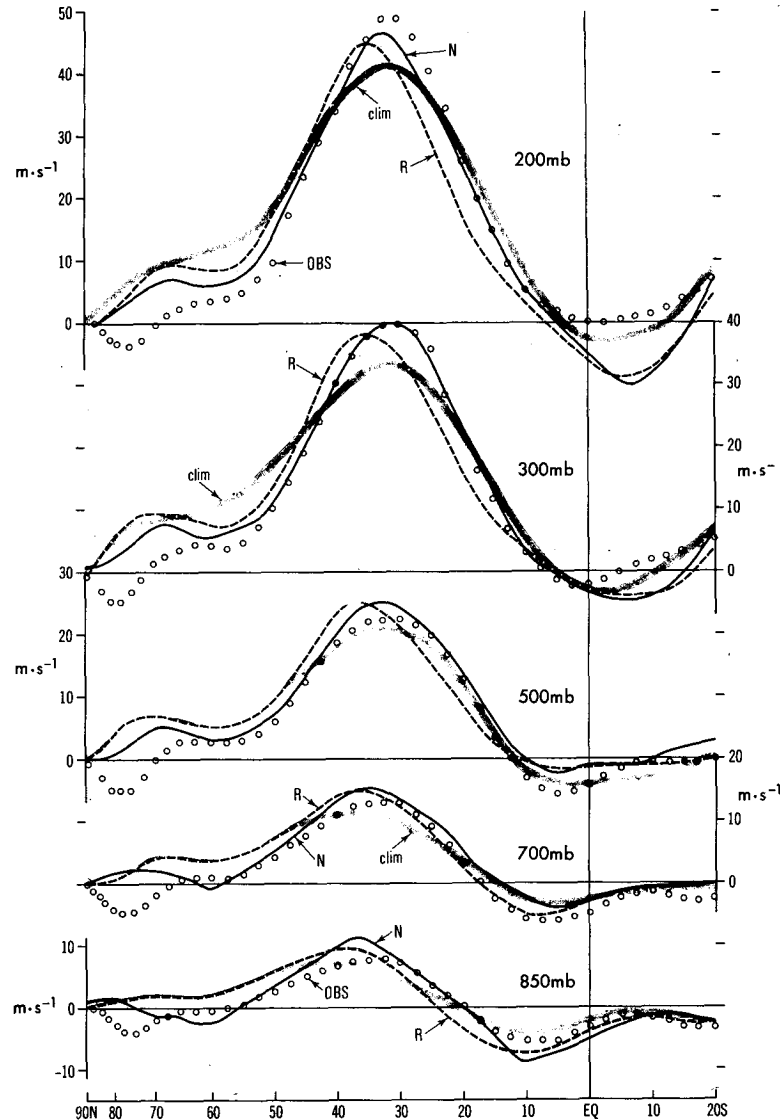
FIG. 15. Zonal winds, averaged monthly and zonally, for the NE (solid line), RA (dashed line), the observation (small circle), and climatology (blurred line). The abscissa is latitude.

ocean temperature and/or snow deposit. In other words, this sort of consideration may be essential for a seasonal forecast but not for a monthly forecast.

c. The mechanisms of the blocking action

Recently, as resonance or multiple equilibrium theories have been proposed as the mechanism of blocking by a number of investigators (e.g., Egger, 1978; 1979; Charney and DeVore, 1979; Hart, 1979; Tung and Lindzen, 1979; Charney and Straus, 1980; Davey, 1980; Trevisan and Buzzi, 1980; Charney et al. 1981; Malguzzi and Speranza, 1981; Kållen, 1982). These theories all deal with the stationary solution or equilibrium state associated with some ex-

treme forcing. Also there is a resonance criterion for the external forcing. The circulation may be either of the blocking type or zonal type, depending upon whether the basic flow is sub-resonant or super-resonant. Orographic forcing is invariably included as a necessary factor for the resonance or near-resonance mechanism. As a result, the extremely meandering or blocking type flow is generated in the lee of the mountain. For Pacific blocks, the Himalayas are supposed to serve as the source of the orographic form drag in these theories.

Our problem is quite different from the above class of stationary problems, because it is a one-month forecast, i.e., an initial value problem. Here, the initial condition rather than the external forcing contains
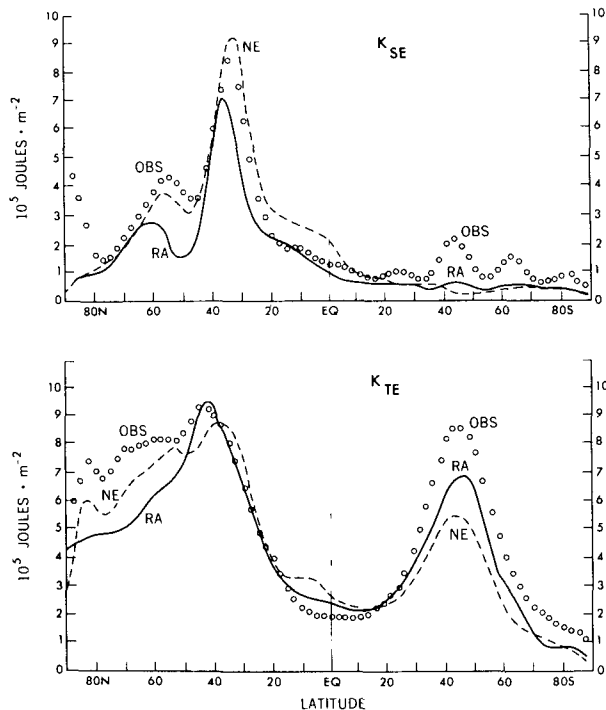
FIG. 16. Stationary and transient eddy kinetic energy K_{SE} and K_{TE} for the NE (dashed), RA (solid) and the observation (small circle), averaged monthly, zonally and vertically. The abscissa is latitude.

the decisive elements for the maintenance and/or the development of blocking. In this sense, our problem is similar to that of Colucci *et al.* (1981), who discussed the "triad resonant interaction" among planetary waves in the absence of external forcings, and is also similar to that of Kalnay and Merkine (1981), who proposed a "local resonant interaction" between the pre-existing orographic flow and the upstream small scale disturbances.

There is a further complication to our problem. Starting with the same initial condition, the simulations were different in the NE and the RA forecasts, for example. As Egger (1978) did, it may be interesting at this stage to see how the *u*-component of wind in the two different models, i.e., the NE and the RA, is distributed with latitude in the sector of 150°E–80°W. Fig. 17 illustrates the monthly mean zonal wind at 500 mb for the observation, the NE and RA predictions and climatology. Clearly, at 40–55°N, the RA wind is far more intense than the NE or the observed. This result agrees with the findings of Hartmann and Ghan (1980), who utilized synoptic analyses of observed maps. They stated that the reduction in local zonal wind intensity accounts for the sharply reduced vorticity tendency associated with blocks. The discrepancy between the RA and NE predicted January 1977 monthly mean zonal flow occurred due to differences in the two GCM's as opposed to differences in external forcing. The poten-

tially most important GCM-dependent factors include spatial resolution, SGS processes and the height of the mountainous terrain.

Fig. 18 shows the relation between the upstream zonal flow and the intensity of the blocks in the case of NE and RA. It may be noted that the weakening of the upstream zonal flow tends to coincide with the intensification of the blocks, and the increase of the upstream flow tends to coincide with the eastward displacement of downstream troughs. The time lag is about 3–4 days for the zonal flow at 120°E–150°W and 35–50°N to affect the downstream ridge at 140°W–100°W and 40–60°N. Admittedly, however, the agreement could be better, particularly for the NE. The reason may be that other mechanisms are superimposed. For example, as was discovered by Charney *et al.* (1981), the blocking ridge is amplified by the passage of a slowly westward propagating global wave pattern. This wave is prominent poleward of 50°N and has a period O (16 days). (Kubota and Iida, 1954; Deland, 1964; Eliasen and Machenhauer, 1965; Madden, 1979).

Apart from this complication, the coincidence between the upstream flow and the downstream block may support the hypothesis that a local resonant interaction exists in the area of Alaska and the rest of the Pacific. It is thus postulated that *a blocking high develops if the zonal wind upstream of the ridge is appropriate, i.e., if there exists a zero or near zero in the local phase speed for a ridge of ~60° longitude width* ("the locally reduced intensity of westerlies"; see the similar observation of Egger, 1978).

There is another possible important effect associated with the local resonant interaction. The effect was theorized for the formation of blocks by Kalnay and Merkine (1981), and by Kållen (1982) in terms of wave forcing. This theory may have some relevance with that of Mahlman (1980), which was mentioned earlier. Kalnay and Merkine discussed that a zonal flow impinging on a narrow isolated mountain barrier with a repeatedly excited perturbation upstream may generate the blocks depending upon the friction intensity and the local resonant condition.

The position of the upstream disturbance appears very crucial. In our case, the barrier for the Pacific block corresponds to the Alaskan mountains and Rockies, and the upstream disturbance location corresponds to the eastern flank of the Aleutian low (the transient eddy amplitude was statistically significant in this region as was mentioned earlier).

In Section 5, the *modon* type pattern was mentioned. This configuration did not exist throughout the whole blocking period, but once it occurred, the stability of the blocking ridge appears to be strengthened. It is interesting to note, however, that the cyclonic pattern in the southern portion of the block is not stationary; new cyclones are intermittently formed and advected eastward. Lau (1979) studied
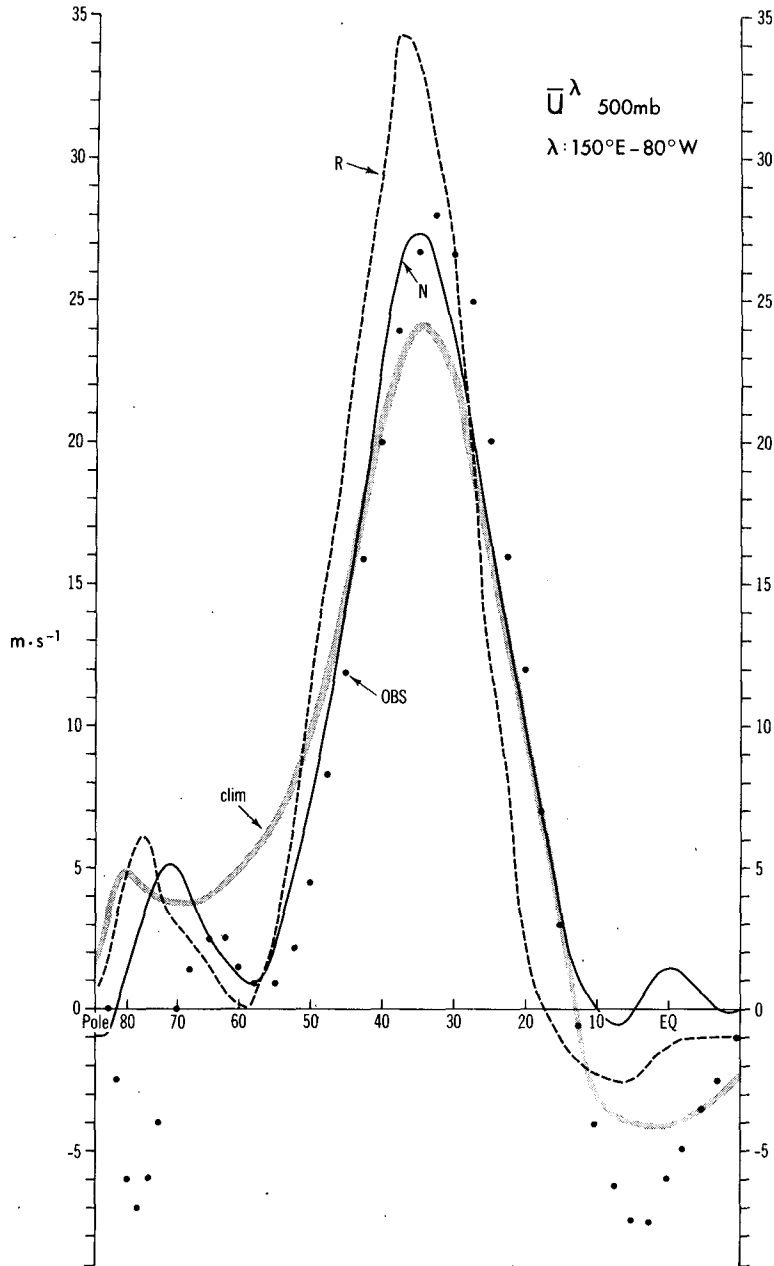
FIG. 17. Zonal winds at 500 mb, that were averaged zonally from 150°E to 80°W, for the NE (solid line), the RA (dashed line), observation (small circle) and climatology (blurred line).

the vorticity balance in terms of the vorticity equation and computed the relative contribution of the stationary and transient motions to the vorticity budget. In Lau's results of 11 winter cases, the contribution of the transient component is relatively smaller than that of the stationary component. Yet the former can be locally substantial as over the Alaskan area. Thus, it is very likely that the transient eddies may be essential for the intensification of the amplitude and the maintenance of stability of the blocks.

7. Conclusions

The uniqueness of this paper is that a real blocking case was treated by a GCM as an initial value problem in the context of a monthly weather forecasting problem.

The one month duration of an extraordinary blocking episode in January 1977 was simulated, to a reasonable extent, by a GCM. The subgrid-scale processes appear important for a satisfactory simu-
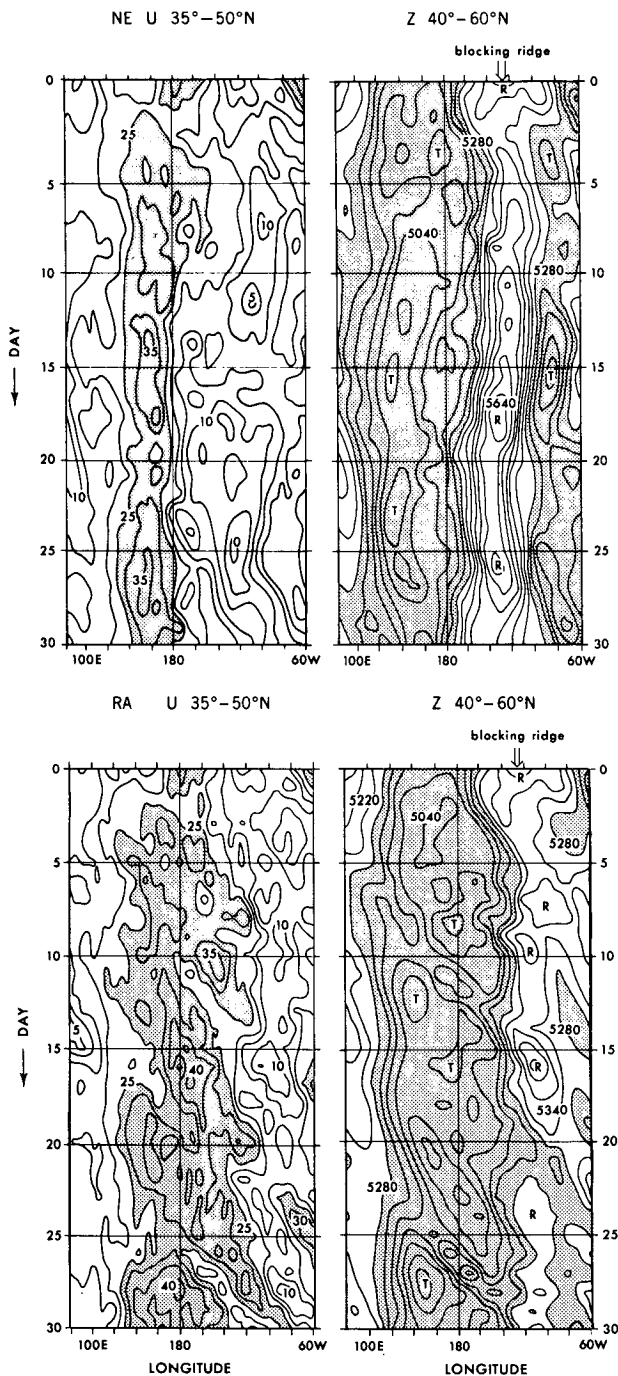
NE U 35°–50°N   Z 40°–60°N

RA U 35°–50°N   Z 40°–60°N

FIG. 18. The relations between the upstream zonal flow (m s⁻¹) and the intensity of blocking ridge are shown by the longitude-time charts of the intensity of zonal component of wind (left) and the geopotential height (m) (right) for the NE prediction (upper) and RA prediction (lower). Areas of wind intensity > 25 m s⁻¹ and areas of geopotential height < 5280 m are shaded. In the geopotential height chart, R and T indicate the ridge and trough, respectively.

lation of maintenance of blocking action at least in this case. Appreciable meandering of the westerlies at middle latitudes was well reproduced by a GCM with advanced physics.

A large number of simulation experiments were carried out. Among them, the poorest performance was experienced by a spectral model with ~660 km × 330 km space resolution (longitude and the meridional directions, respectively) and the conventional, 1965 GFDL physics package. The most successful model was a finite difference model with 440 km × 240 km space resolution and advanced physics. The advanced physics package is similar to the conventional physics package except that it incorporates a turbulent closure scheme for subgrid-scale vertical transport, surface flux schemes based on the Monin–Obukhov similarity theory and soil heat conduction and excludes dry convective adjustment.

In the most successful experiment, the zonal westerlies were weaker than normal at high latitudes upstream of the blocking ridge, and the westerly maxima were shifted equatorward and were stronger than normal. It is speculated that this condition may be favorable for maintaining a solitary blocking ridge.

It may be asked if the "superior model" remains more capable than the "inferior model" at simulating any other blocking case. This question cannot be answered yet. But further studies are in progress to assess the performance of various SGS processes for six cases of monthly prediction.

APPENDIX

A Comparison of Maps From Various Model Forecasts

By selecting geopotential height maps for an instantaneous time, day 10, and for the 5-day mean, i.e., day 25–30, the impact of various GCM's on the numerical simulation is displayed. The models chosen here are four different kinds, i.e., R30L9-A2, R30L9-E4, N48L9-A2 and N48L9-E4.

Fig. A1 is the map of day 10 for 500 mb geopotential height. Figure A2 is the map for day 25–30. The difference of height patterns between the models was not very great at day 10, but the difference became quite substantial for day 25–30. These figures may indicate that the results of the spectral models are similar to each other, and likewise, those of the finite difference models are similar to each other, and that a common characteristic may be noticed among forecasts which used the same physics package. The E4 physics tends to maintain the large meandering of westerlies better than the A2 physics.
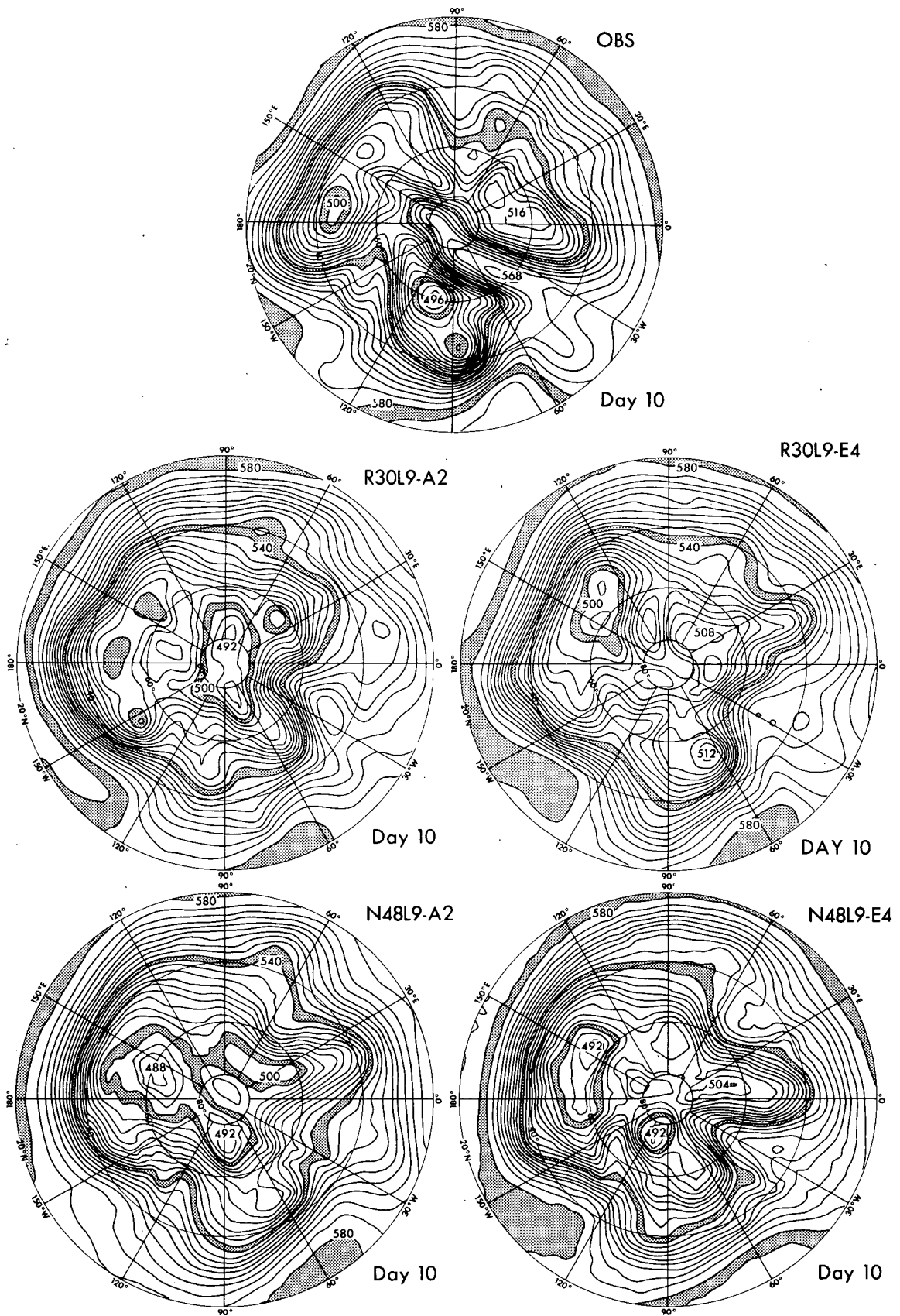
FIG. A1. The 500 mb geopotential height maps of the observation and four model prognoses at day 10 (0000 GMT 11 January 1977) for the Northern Hemisphere poleward of 20°N. Contour interval is 40 m. Belts of height contours between 5000–5040, 5400–5440 and 5800–5840 m are shaded to enhance the patterns.
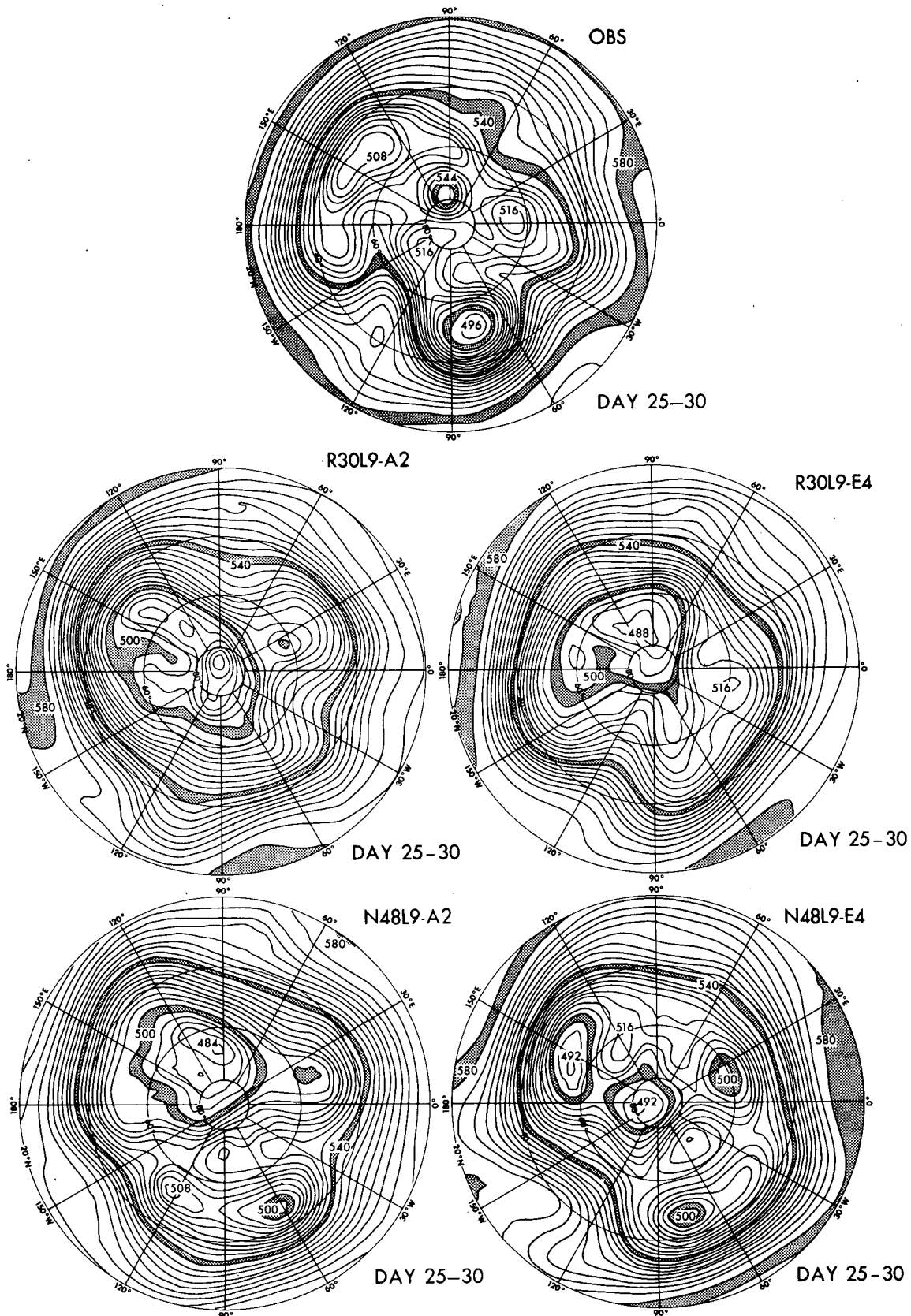
FIG. A2. As is Fig. A1, but for the 5-day mean of Day 25–30.

REFERENCES

Alexander, R. C., and R. I. Mobley, 1976: Monthly average sea-surface temperature and ice-pack limits on a 1° global grid. *Mon. Wea. Rev.*, **104**, 143–148.

Austin, J. F., 1980: The blocking of mid-latitude westerly winds by planetary waves. *Quart. J. Roy. Meteor. Soc.*, **106**, 327–350.

Bengtsson, L., 1981: Numerical prediction of atmospheric blocking—case study. *Tellus*, **33**, 19–42.

Bourke, W., 1974: Multi-level spectral model. I. Formulation and hemisphere integrations. *Mon. Wea. Rev.*, **102**, 687–701.

——, B. J. McAvaney, K. Puri, and R. Thurling, 1977: Global modelling of atmospheric flow by spectral methods. *Methods in Computational Physics*, Vol. 17, *General Circulation Models of the Atmosphere*, J. Chang, Ed., Academic Press, 267–324.

Charney, J., and J. DeVore, 1979: Multiple flow equilibria in the atmosphere and blocking. *J. Atmos. Sci.*, **36**, 1205–1216.

——, and P. M. Straus, 1980: Form-drag instability multiple equilibria and propagating planetary waves in baroclinic orographically forced, planetary wave system. *J. Atmos. Sci.*, **37**, 1157–1176.

——, J. Shukla and K. C. Mo, 1981: Comparison of a barotropic blocking theory with observation. *J. Atmos. Sci.*, **38**, 762–779.

Colucci, S. J., A. Z. Loesch and L. F. Bosart, 1981: Spectral evolution of a blocking episode and comparison with wave interaction theory. *J. Atmos. Sci.*, **38**, 2092–2111.

Davey, M. K., 1980: A quasi-linear theory for rotating flow over topography. Part 2. Beta-plane annulus. *J. Fluid Mech.*, **103**, 297–320.

Davies, D. R., 1978: Blocking anticyclones. *Weather*, **33**, 30–32.

Deland, R. J., 1964: Travelling planetary scale waves. *Tellus*, **16**, 271–273.

Edmon, H. J., 1980: A study of the general circulation over the Northern Hemisphere during the winters 1976–1977 and 1977–1978. *Mon. Wea. Rev.*, **108**, 1538–1553.

Egger, J., 1978: Dynamics of blocking highs. *J. Atmos. Sci.*, **35**, 1788–1801.

——, 1979: Stability of blocking in barotropic channel flow. *Beitr. Phys. Atmos.*, **52**, 27–43.

Eliasen, E., and B. Machenhauer, 1965: A study of the fluctuations of the atmospheric planetary flow patterns represented by spherical harmonics. *Tellus*, **17**, 220–238.

Epstein, E. S., 1969: Stochastic dynamic prediction. *Tellus*, **21**, 739–759.

Everson, P. J., and D. R. Davies, 1970: On the use of a simple two-level model in general circulation studies. *Quart. J. Roy. Meteor. Soc.*, **96**, 404–413.

Flattery, T. W., 1971: Spectral models for global analysis and forecasting. *Proc. Sixth AWS Tech. Exch. Conf.*, U.S. Naval Academy, 21–24 September 1970. Air Weather Service Tech. Rep. 242, 42–54.

Fleming, R. J., 1971: On stochastic dynamic prediction: II. Predictability and utility. *Mon. Wea. Rev.*, **99**, 927–938.

Gordon, C. T., and W. Stern, 1974: Spectral modelling at GFDL. *The GARP Programme on Numerical Experimentation—Report Int. Symp. Spectral Methods in Numerical Weather Prediction for GARP*, Copenhagen, WMO/GARP Rep. No. 7, 46–80.

——, and ——, 1982: A description of the GFDL global spectral model. *Mon. Wea. Rev.*, **110**, 625–644.

Hart, J., 1979: Barotropic quasi-geostrophic flow over anisotropic mountains. *J. Atmos. Sci.*, **36**, 1736–1746.

Hartmann, D. L., and S. J. Ghan, 1980: A statistical study of the dynamics of blocking. *Mon. Wea. Rev.*, **108**, 1144–1159.

Horel, J. D., and J. M. Wallace, 1981: Planetary-scale atmospheric phenomena associated with the Southern Oscillation. *Mon. Wea. Rev.*, **109**, 813–829.

Hoskins, B. J., and D. J. Karoly, 1981: The steady linear response of a spherical atmosphere to thermal and orographic forcing. *J. Atmos. Sci.*, **38**, 1179–1196.

Jarraud, M., D. Girard and U. Cubasch, 1981: Comparison of medium range forecasts made with models using spectral or finite difference techniques in the horizontal. Tech. Rep. No. 23, European Centre for Medium Range Weather Forecasts, 95 pp.

Kållen, E., 1982: Bifurcation properties of quasi-geostrophic, barotropic models and their relation to atmospheric blocking. *Tellus*, **34**, 255–265.

Kalnay-Rivas, E., and L. O. Merkine, 1981: A simple mechanism for blocking. *J. Atmos. Sci.*, **38**, 2077–2091.

Kikuchi, Y., 1969: Numerical simulation of the blocking process. *J. Meteor. Soc. Japan*, **47**, 29–54.

——, 1971: Influence of mountains and land–sea distribution on blocking action. *J. Meteor. Soc. Japan*, **49**, 137–155.

——, 1979: The influence of orography and land–sea distribution on winter circulation. *Pap. Meteor. Geophys.*, **30**, 1–32.

Krueger, A. F., J. S. Winston and D. A. Haines, 1965: Computations of atmospheric energy and its transformation for the Northern Hemisphere for a recent five year period. *Mon. Wea. Rev.*, **93**, 227–238.

Kubota, S., and S. Iida, 1954: Statistical characteristics of the atmospheric disturbances. *Pap. Meteor. Geophys.*, **5**, 22–34.

Lau, N-C., 1979: The observed structure of tropospheric stationary waves and the local balances of vorticity and heat. *J. Atmos. Sci.*, **36**, 996–1016.

Leith, C. E., 1974: Theoretical skill of Monte Carlo forecasts. *Mon. Wea. Rev.*, **102**, 409–418.

Lejenäs, H., 1977: On the breakdown of the westerlies. *Atmosphere*, **15**, 89–113.

Madden, R. A., 1979: Observations of large-scale traveling Rossby waves. *Rev. Geophys. Space Phys.*, **17**, 1935–1949.

Mahlman, J. D., 1980: Structure and interpretation of blocking anticyclones as simulated in a GFDL general circulation model. *Proc. Thirteenth Stanstead Seminar*, Quebec, Canada. Dept. Meteor. McGill University, 70–76.

Malguzzi, P., and A. Speranza, 1981: Local multiple equilibria and regional atmospheric blocking. *J. Atmos. Sci.*, **38**, 1939–1948.

Manabe, S., J. Smagorinsky and R. Strickler, 1965: Simulated climatology of a general circulation model with a hydrological cycle. *Mon. Wea. Rev.*, **93**, 765–798.

——, D. G. Hahn, and J. L. Holloway, Jr., 1974: The seasonal variation of the tropical circulation as simulated by a global model of the atmosphere. *J. Atmos. Sci.*, **31**, 43–83.

McWilliams, J. C., 1980: An application of equivalent modons to atmospheric blocking. *Dyn. Atmos. Oceans*, **5**, 43–66.

Miyakoda, K., and J. Sirutis, 1977: Comparative integrations of global models with various parameterized processes of subgrid-scale vertical transports: Description of the parameterizations. *Contrib. Atmos. Phys.*, **50**, 445–487.

——, and R. F. Strickler, 1981: Cumulative results of extended forecast experiment. Part III: Precipitation. *Mon. Wea. Rev.*, **109**, 830–842.

——, and J. P. Chao, 1982: Essay on dynamical long-range forecasts of atmospheric circulation. *J. Meteor. Soc. Japan*, **60**, 292–307.

Namias, J., 1978: Multiple causes of the North American abnormal winter 1976–77. *Mon. Wea. Rev.*, **106**, 279–295.

National Academy of Sciences, 1966: The feasibility of a global observation and analysis experiment. Publ. 1290, NAS-NRC, Washington, DC, 172 pp.

O'Neill, A., and B. F. Taylor, 1979: A study of the major stratospheric warming of 1976–77. *Quart. J. Roy. Meteor. Soc.*, **105**, 71–92.

Palmén, E., and C. W. Newton, 1969: *Atmospheric Circulation Systems. International Geophysics Series*, Vol. 13, Academic Press, 603 pp.

Quiroz, R. S., 1977: The tropospheric stratospheric polar vortex breakdown of January 1977. *Geophys. Res. Lett.*, **4**, 151–154.

Rex, D. P., 1950: Blocking action in the middle troposphere and its effect upon regional climate. II. The climatology of blocking action. *Tellus*, **2**, 275–301.

——, 1951: Blocking activity in the middle troposphere and its effect upon regional climate. *Tellus,* **2,** 275–301.

Shukla, J., 1981: Dynamical predictability of monthly means. *J. Atmos. Sci.,* **38,** 2547–2572.

Simmons, A. J., 1981: Tropical influences on stationary wave motion in middle and high latitudes. European Centre for Medium Range Weather Forecasts, Tech. Rep. No. 26, 57 pp.

Smagorinsky, J., 1963: General circulation experiments with the primitive equations. I: The basic experiment. *Mon. Wea. Rev.,* **91,** 99–164.

——, 1969: Problems and promises of deterministic extended range forecasting. *Bull. Amer. Meteor. Soc.,* **50,** 286–311.

Spar, J., J. J. Nortario and W. J. Quirk, 1978: An initial state perturbation experiment with the GISS model. *Mon. Wea. Rev.,* **106,** 89–106.

Taylor, B. F., and J. D. Perry, 1977: The major stratospheric warming of 1976–77. *Nature,* **267,** 417–418.

Trevisan, A., and A. Buzzi, 1980: Stationary response of barotropic weakly nonlinear Rossby waves to quasi-resonant orographic forcing. *J. Atmos. Sci.,* **37,** 947–959.

Tung, K. K. and R. S. Lindzen, 1979: A theory of stationary long waves. Part I: A simple theory of blocking. Part II: Resonant Rossby waves in the presence of realistic vertical shear. *Mon. Wea. Rev.,* **107,** 714–750.

Umscheid, L., Jr., and P. R. Bannon, 1977: A comparison of three global grids used in numerical prediction models. *Mon. Wea. Rev.,* **105,** 618–635.

U.S. Dept. of Commerce and U.S. Dept. of Agriculture, 1977: National weather summary. *Weekly Wea. Crop Bull.,* **64,** Nos. 1–5.

Wagner, A. J., 1977: Weather and Circulation of January 1977— The coldest month on record in the Ohio Valley. *Mon. Wea. Rev.,* **105,** 553–560.

Wallace, J. N., and D. S. Gutzler, 1980: Teleconnections in the geopotential height field during the Northern Hemisphere winter. *Mon. Wea. Rev.,* **109,** 784–812.

——, S. Tibaldi and A. J. Simmons, 1983: Reduction of systematic forecast errors in the ECMWF model through the introduction of an envelope orography. Submitted to *Quart. J. Roy. Meteor. Soc.*

White, W. B., and N. E. Clark, 1975: On the development of blocking ridge activity over the central North Pacific. *J. Atmos. Sci.,* **32,** 489–502.

Yeh, T-C. 1949: On energy dispersion in the atmosphere. *J. Meteor.,* **6,** 1–16.